EEET ECOLOGICAL ENGINEERING & ENVIRONMENTAL TECHNOLOGY

Ecological Engineering & Environmental Technology, 2026, 27(9), 37–50
https://doi.org/10.12912/27197050/225814
ISSN 2719–7050, License CC-BY 4.0

Received: 2026.07.03
Accepted: 2026.07.30
Published: 2026.08.15

Pro-ecological microwave-assisted extraction of phytochemicals from *Moringa oleifera* Lam. leaves: Multi-response surface optimization and predictive modeling

Thanh-Binh Huynh[1,2], Thuy-Cam-Tu Nguyen[1,2], Thi-An-Sa Do[1,2], Trung Dang-Bao[1,2*]

[1] Analytical Chemistry and Sustainability Trends Research Group, Faculty of Chemical Engineering, Ho Chi Minh City University of Technology, 268 Ly Thuong Kiet Street, Dien Hong Ward, Ho Chi Minh City, Vietnam
[2] Vietnam National University Ho Chi Minh City, Linh Xuan Ward, Ho Chi Minh City, Vietnam
* Corresponding author's e-mail: dbtrung@hcmut.edu.vn

ABSTRACT

This study presents a pro-ecological approach for the efficient recovery of natural antioxidants from plant matrixes by optimizing the green microwave-assisted extraction (MAE) of bioactive compounds from *Moringa oleifera* Lam. leaves. A central composite design (CCD) coupled with response surface methodology (RSM) was employed to model and evaluate extraction performance as a function of eco-friendly process parameters: ethanol concentration (X_1, % v/v), liquid-to-solid ratio (X_2, mL g^{-1}), and extraction time (X_3, s). The predictive response models effectively mapped three independent targets: total phenolic content (TPC, Y_1), total flavonoid content (TFC, Y_2), and reducing sugar content (RSC, Y_3). The individual optimal conditions (X_1, X_2, X_3) to maximize yields were successfully determined to be (40% v/v, 50:1 mL g^{-1}, 85 s) for TPC, (60% v/v, 50:1 mL g^{-1}, 90 s) for TFC, and (20% v/v, 45:1 mL g^{-1}, 100 s) for RSC. Under these respective parameters, experimental maximums reached 23.5 mg GAE/g, 20.8 mg RE/g, and 76.3 mg GE/g, closely validating the predictive simulations. Strong positive correlations were observed between antioxidant activity (AA) and both TPC ($R^2 = 0.78$) and TFC ($R^2 = 0.73$). These findings demonstrate that optimized MAE serves as an energy-saving and sustainable bioprocess for isolating high-value phytochemicals with minimal environmental impact.

Keywords: *Moringa oleifera* Lam., green extraction, pro-ecological technology, response surface methodology, process optimization, bioactive compounds, antioxidant activity.

INTRODUCTION

Natural flora synthesizes an array of primary and secondary metabolites, collectively termed phytochemicals, which play an indispensable role in human health promotion (Dahmoune et al., 2015; Chatepa et al., 2025). Among these bioactives, flavonoids and phenolic constituents are highly regarded for their robust antioxidant capacities (Chatepa et al., 2025; Alara et al., 2021; Huynh et al., 2025). By neutralizing oxidative stress, these specific molecules offer vital defense mechanisms against a spectrum of chronic pathologies, including metabolic disorders, obesity, malignancies, and cardiovascular diseases (Szopa et al., 2024; Filip et al., 2017; Khatri and Chhetri, 2020). At a physiological level, they contribute significantly to lowering systemic blood pressure and enhancing endothelial performance (Vijayalaxmi et al., 2014; Hu et al., 2022). Consequently, plant-derived bioactive extracts have found widespread utility as functional ingredients across the pharmaceutical, nutraceutical, cosmetic, and food industries (Yang and Hong, 2018; Lama-Calvente et al., 2024).

Within the Moringaceae family, *Moringa oleifera* Lam. (*M. oleifera* L.) stands out as a globally cultivated species renowned for its versatile nutritional, agricultural, and therapeutic applications (Gao et al., 2025; Gharsallah et al., 2023; Zhu et al., 2020). This botanical matrix possesses an extensive array of essential macronutrients

and micronutrients, including proteins, vitamins, and minerals, paired with a rich diversity of secondary metabolites such as tannins, saponins, alkaloids, sterols, terpenoids, phenols, and flavonoids (Chatepa et al., 2025; Hamid et al., 2025). Although virtually every part of the plant, ranging from roots and stems to seeds and pods, has been investigated for its functional or medicinal purposes (Gao et al., 2025; Gharsallah et al., 2023), the leaves remain the primary focus of utilization. This preference stems from their high nutritional density (Zhu et al., 2020) and their concentrated profile of specific bioactive compounds that drive strong radical scavenging performance (Wei et al., 2023; Peng et al., 2025; Teclegeorgish et al., 2021).

The ultimate phytochemical profile of *M. oleifera* L. depends heavily on postharvest and processing variables, such as drying conditions, extraction techniques, solvent types, and contact times (Bennour et al., 2021; Chokoe et al., 2025; Rodríguez-Pérez et al., 2015). To date, several conventional and advanced extraction frameworks have been applied to map these bioactives. For instance, Rodríguez-Pérez et al. (2015) evaluated how maceration compared against ultrasound-assisted extraction (UAE) using water, acetone, methanol, and ethanol for Madagascar-grown samples. Similarly, Gao et al. (2025) screened eight distinct organic solvents under UAE conditions to explore the neuroprotective and antioxidant traits of Chinese *M. oleifera* L. More recently, deep eutectic solvents have been paired with both UAE and conventional maceration to isolate phenolics (Chatepa et al., 2025; Wei et al., 2023; Wu et al., 2020). Despite their efficacy, scaling up these classical or ultrasound-based protocols often introduces commercial and environmental bottlenecks, including high energy demands, excessive waste generation, and prolonged processing windows. To mitigate these drawbacks, microwave-assisted extraction (MAE) has garnered interest as a sustainable, rapid, and economical alternative (Tomasi et al., 2023; Bouras et al., 2015; Al-Shalabi et al., 2024). MAE significantly accelerates mass transfer while minimizing solvent volumes, thereby optimizing the recovery efficiency of target antioxidants.

In Vietnam, the systematic exploitation of *M. oleifera* L. is still in its infancy, and there remains a noticeable literature gap regarding the deployment of MAE coupled with response surface methodology (RSM) for processing domestic cultivars. Addressing this deficit, the present study focuses on leveraging MAE to maximize the extraction efficiency of *M. oleifera* L. polyphenols, specifically tracking total phenolic content (TPC), total flavonoid content (TFC), reducing sugar content (RSC), and overall antioxidant activity (AA). Furthermore, a central composite design (CCD) under an RSM framework was implemented to mathematically optimize the recovery process and unravel the interrelationships among these co-extracted bioactives. While MAE efficiency is generally governed by variable arrays like irradiation power, temperature, extraction time, liquid-to-solid ratio (L/S), and solvent systems (Tomasi et al., 2023; Pimentel-Moral et al., 2018), this work utilized an aqueous ethanol (EtOH) binary mixture due to its strong dielectric properties and high affinity for polar aromatics (Al-Shalabi et al., 2024; Pimentel-Moral et al., 2018). Specifically, the optimization model evaluated three independent operational factors (EtOH concentration, L/S ratio, and extraction duration) while maintaining constant microwave power and temperature settings.

EXPERIMENTAL

Chemicals and methods

Sigma-Aldrich (Germany) was the source for all primary analytical standards and reagents, including Trolox, rutin, gallic acid, D-glucose, potassium sodium tartrate, 3,5-dinitrosalicylic acid (DNSA), 2,2-diphenylpicrylhydrazyl (DPPH), aluminum chloride hexahydrate, and the Folin-Ciocalteu reagent.

Fresh *M. oleifera* L. leaves were harvested from rural regions located in Tay Ninh Province, Vietnam. To remove surface contaminants, the collected biomass was rinsed thoroughly with water. The clean leaves were subsequently dehydrated in a forced-air oven maintained at 50 °C until a stable, constant weight was achieved. Following dehydration, the sample matrix was pulverized into a fine, homogeneous powder, packed securely inside airtight polyethylene bags, and stored under dark conditions in a refrigerator at 4 °C to prevent phytochemical degradation prior to extraction.

To evaluate the impacts of three independent operational variables, namely EtOH concentration (% v/v), L/S ratio (mL g^{-1}), and irradiation time (s), on the extraction yields of TPC, TFC, and RSC, individual extraction trials were carried

out in triplicate. A central composite design (CCD) matrix dictated the precise multi-factor combinations for each experimental run. Methodologically, a fixed mass of 0.50 g of processed *M. oleifera* L. leaf powder was introduced into the microwave reaction vessels and thoroughly suspended in pre-calculated volumes of the designated aqueous ethanol solvent. The irradiation treatment was executed utilizing a microwave system (22 L volume capacity, Panasonic, Japan) configured to a constant output power level to guarantee thermal uniformity throughout the specified processing intervals. Upon completion of the heating cycles, vacuum filtration was applied to separate the spent biomass from the liquid phase, and the gathered filtrates were stored for downstream quantification of TPC, TFC, RSC, and AA.

The TPC was determined using the Folin-Ciocalteu assay (Dahmoune et al., 2015). Operationally, a 0.50 mL aliquot of the appropriately diluted leaf extract was reacted with 2.50 mL of a 10% Folin-Ciocalteu working solution. Following a brief 5-minute equilibration period, the reaction was stabilized by adding 2.00 mL of a 7.5% aqueous sodium carbonate solution. The resulting mixture was then left to incubate under dark conditions at ambient temperature for exactly 60 minutes. Subsequently, the solution absorbance was recored at 765 nm utilizing a UV-Vis spectrophotometer (Libra S22, Biochrom). Gallic acid served as the calibration reference standard ($y = 0.0109x + 0.0149$, $R^2 = 0.9984$), with final values expressed as milligrams of Gallic Acid Equivalents per gram of dry plant material (mg GAE/g).

The TFC was assessed following a modified aluminum chloride colorimetric method (Nguyen-Doan et al., 2024). In brief, a 1.00 mL volume of the diluted sample was combined sequentially with 0.30 mL of a 5% sodium nitrite solution, 0.30 mL of 10% aluminum chloride hexahydrate, and 2.00 mL of a 1.0 M sodium hydroxide solution. Deionized water was then added to bring the ultimate solution volume to exactly 10.00 mL. After allowing the chemical system to achieve equilibrium for 10 minutes, the absorbance was monitored at 510 nm against an appropriate reagent blank. A calibration curve prepared from rutin was utilized for quantification ($y = 0.0014x + 0.0009$, $R^2 = 0.9986$), and results were translated to milligrams of Rutin Equivalents per gram of dry weight sample (mg RE/g).

The RSC was determined by adapting the DNSA colorimetric method (Wood et al., 2012; Lam et al., 2021). The protocol involved blending 2.00 mL of the prepared leaf extract with an identical volume (2.00 mL) of the DNSA working reagent inside a standard glass test tube. The combined matrix was subsequently incubated in a water bath held at 80 °C for a duration of 10 minutes. Once cooled completely to room temperature, distilled water was mixed in to achieve a final target volume of 10.00 mL. The optical density of the solution was scanned at 540 nm. D-glucose was employed to establish the standard calibration curve ($y = 0.0035x – 0.0671$, $R^2 = 0.9951$), and the calculated reducing capacity was specified as milligrams of D-glucose Equivalents per gram of dry powder (mg GE/g).

The overall AA was measured by tracking their capacity to reduce the DPPH radical, following the foundational methodology of Bouras et al. (2015). For this assay, a 1.00 mL portion of the diluted sample was transferred into a clean test tube and directly combined with 2.00 mL of a 0.1 mM ethanolic DPPH solution. The reaction environment was maintained in absolute dark at room temperature for an incubation window of 30 minutes. Following this, the remaining radical concentration was quantified by measuring the absorbance at 517 nm. Trolox was used as the benchmark reference standard ($y = 5.4740x + 0.0947$, $R^2 = 0.9921$), with the final antioxidant activity values expressed as milligrams of Trolox Equivalents per gram of dry sample mass (mg TE/g).

Experimental design and statistical analysis

To model processing conditions, evaluate the impacts of critical operational variables, and determine the optimal windows for the MAE process, RSM driven by a CCD serves as an effective statistical tool (Izadiyan and Hemmateenejad, 2016; Azahar et al., 2017). In the present work, JMP statistical software (version 18.2.1) was utilized to generate the experimental matrix, execute data analysis, and construct the predictive mathematical equations (Huynh et al., 2025). Optimization of the extraction process was achieved via a five-level CCD framework, which evaluated three independent factors: EtOH concentration (X_1, 10 - 60 % v/v), L/S ratio (X_2, 20:1 - 60:1 mL g^{-1}), and microwave irradiation duration (X_3, 60 - 120 s). The corresponding dependent target responses tracked were TPC (Y_1, mg GA/g), TFC (Y_2, mg RE/g), and RSC (Y_3, mg

GE/g). Table 1 outlines the complete operational ranges and codified levels of the investigated independent variables.

To model the experimental data of the targeted dependent responses, a multi-variable regression analysis was executed to construct the corresponding second-order polynomial equation, expressed below as Equation 1 (Tomasi et al., 2023).

$$Y = \beta_0 + \sum_{i=1}^{k} \beta_i X_i + \sum_{i=1}^{k-1} \sum_{j=i+1}^{k} \beta_{ij} X_i X_j + \sum_{i=1}^{k} \beta_{ii} X_i^2 \quad (1)$$

where: Y represents the predicted response; X_i and X_j are the independent variables; β_0, β_i, β_{ii}, and β_{ij} are the regression coefficients for intercept, linear, quadratic, and interaction terms, respectively, and k is the number of independent parameters (k = 3).

To validate the reliability and goodness-of-fit of the constructed response models, analysis of variance (ANOVA) was systematically executed. Model adequacy was verified by examining a suite of diagnostic statistical criteria, namely the lack-of-fit feature, the coefficient of variation (C.V.%), the adjusted determination coefficient (R^2_{adj}), and the overall coefficient of determination (R^2). High regression F-values paired with a significance threshold of $p < 0.05$ served as the benchmark to confirm the statistical validity of the models. Furthermore, to provide a clear visual interpretation of the interactive dynamics between the independent operational variables and the targeted extraction outputs, the fitted second-order polynomial equations were translated into three-dimensional (3D) response surface plots.

RESULTS AND DISCUSSION

Statistical modeling and analysis of variance

To minimize biological and batch-to-batch variability of the plant matrix, a single, large collection of dried *M. oleifera* L. leaves was thoroughly pulverized, sieved, and mixed into a uniform, homogenized pool used for all subsequent trials. A central composite design (CCD) coupled with response surface methodology (RSM) was then deployed to comprehensively map how the three operational parameters (EtOH concentration (X_1), L/S ratio (X_2), and extraction time (X_3)) interactively influence the isolation of target bioactives.

Following the specific experimental matrix configurations detailed in Table 1, a total of twenty distinct processing trials (incorporating six identical center-point replicates) were carried out. To eliminate systematic bias and time-dependent experimental errors, the execution order of these trials was fully randomized. Furthermore, all subsequent quantitative analyses, including TPC, TFC, and RSC, were performed in triplicate to ensure analytical precision, with the resulting empirical data consolidated in Table 2.

Table 3 provides a comprehensive breakdown of the calculated analysis of variance (ANOVA) metrics alongside the corresponding regression coefficients for all cross-product interaction, second-order quadratic, and first-order linear terms across each dependent target response.

Statistical analysis for the TPC yield revealed that the linear coefficients for EtOH fraction (X_1) and L/S ratio (X_2), along with their corresponding second-order quadratic terms (X_1^2 and X_2^2), exerted a highly critical influence on the model ($p < 0.0001$). Conversely, processing duration (X_3) displayed a statistically negligible linear impact ($p > 0.05$); however, it exhibited a significant nonlinear relationship via its quadratic term (X_3^2, $p < 0.001$). Regarding cross-product interactions, only the X_1X_2 parameter combination demonstrated a

Table 1. Independent processing variables and their corresponding coded/actual levels established for the CCD

Independent variables		Uncoded values				
Uncoded	Coded	-a (-1.68)	Lower (-1)	Central (0)	Higher (+1)	+a (+1.68)
EtOH concentration	X_1	6.4 [a]; 3.2 [b]	20 [a]; 10 [b]	40 [a]; 20 [b]	60 [a]; 30 [b]	73.6 [a]; 36.8 [b]
L/S ratio	X_2	6.4	20	40	60	73.6
Extraction time	X_3	39.6	60	90	120	140.4

Note: [a] EtOH concentration for the TPC and TFC extraction, [b] EtOH concentration for the RSC extraction.

Table 2. CCD experimental matrix alongside the corresponding empirical values for the three evaluated target responses

Run No.	Coded experimental conditions			Actual responses			Predicted responses		
	X_1	X_2	X_3	Y_1	Y_2	Y_3	Y_1	Y_2	Y_3
1	-a	0	0	16.9	9.1	34.7	17.3	9.4	33.3
2	-1	-1	-1	13.4	7.0	22.0	12.9	7.0	18.0
3	-1	-1	+1	13.0	7.8	21.6	13.3	7.8	26.9
4	-1	+1	-1	22.0	13.3	50.0	21.8	14.0	46.1
5	-1	+1	+1	21.9	14.8	58.8	21.6	13.0	63.6
6	0	-a	0	(-)	(-)	(-)	12.4	5.8	17.2
7	0	0	-a	20.3	17.0	37.8	20.8	15.9	48.7
8	0	0	0	22.3	16.6	73.8	22.5	18.0	75.3
9	0	0	0	22.5	17.0	74.6	22.5	18.0	75.3
10	0	0	0	23.1	19.3	75.9	22.5	18.0	75.3
11	0	0	0	22.9	17.8	73.5	22.5	18.0	75.3
12	0	0	0	22.3	18.7	76.7	22.5	18.0	75.3
13	0	0	0	22.2	19.0	77.2	22.5	18.0	75.3
14	0	0	+a	20.5	14.0	73.1	20.2	16.1	62.6
15	0	+a	0	20.0	14.5	41.8	20.2	15.6	42.2
16	+1	-1	-1	19.0	12.1	39.5	19.1	13.1	34.4
17	+1	-1	+1	18.6	15.9	29.6	18.6	14.4	33.2
18	+1	+1	-1	20.6	20.2	32.9	20.1	19.5	27.3
19	+1	+1	+1	18.7	19.7	31.1	19.0	19.0	34.9
20	+a	0	0	20.5	18.7	21.1	20.4	19.5	22.9

highly pronounced effect ($p < 0.0001$), while the remaining interactive pairings (X_1X_3 and X_2X_3) failed to reach statistical significance ($p > 0.05$). Based on these validated weights, the optimized empirical equation for projecting TPC values (Equation 2) was formulated as follows:

$$Y_1 = -14.872 + 0.524X_1 + 0.860X_2 + \\ + 0.143X_3 - 0.005X_1X_2 - 0.003X_1^2 - \\ - 0.006X_2^2 - 0.001X_3^2 \quad (2)$$

The model's adequacy and predictive capacity were verified evaluating its R^2 and R^2_{adj} (Yang and Hong, 2018). As detailed in the ANOVA data summarized in Table 3, the computed R^2 for the TPC dataset reached 0.9873, signifying that 98.73% of the operational variance captured during the MAE of *M. oleifera* L. polyphenols is mathematically accounted for by the designated independent variables, leaving a negligible residual variation of 1.27% unexplained. Because an elevated R^2 value alone does not definitively establish the robustness of a quadratic framework, a reliable statistical model necessitates that the R^2_{adj} parameter aligns closely with its primary R^2 counterpart (Dahmoune et al., 2015). Adhering to this benchmark, the high degree of parity observed between the R^2 and R^2_{adj} values in Table 3 strongly validates the mathematical fitness of the regression. Furthermore, the C.V.% stood at a low 2.33%, verifying good empirical reproducibility for this target response and confirming that the developed second-order framework is both dependable and highly precise for projecting TPC extraction kinetics.

With respect to the TFC, the statistical analysis indicated that the extraction efficiency was significantly driven by both the linear and second-order quadratic parameters of the EtOH concentration (X_1 and X_1^2) and the L/S ratio (X_2 and X_2^2, $p < 0.05$). In contrast, neither the microwave irradiation time (X_3 and X_3^2) nor any of the cross-product interaction terms (X_1X_2, X_1X_3, and X_2X_3) exerted a meaningful impact on the process, remaining statistically negligible ($p > 0.05$). Consequently, omitting these non-contributing parameters allowed for the formulation of a streamlined, reduced predictive framework, as expressed by Equation 3:

Table 3. Statistical parameters, second-order polynomial regression coefficients, and corresponding analysis of variance (ANOVA) metrics for the evaluated extraction responses

Term	Response											
	Y_1				Y_2				Y_3			
	DF [a]	SS [b]	p-value	F-value	DF [a]	SS [b]	p-value	F-value	DF [a]	SS [b]	p-value	F-value
Linear												
X_1	1	11.56	<0.0001	53.04	1	124.07	<0.0001	50.95	1	130.23	0.1274	2.82
X_2	1	48.51	<0.0001	222.62	1	76.17	0.0003	31.28	1	493.41	0.0097	10.68
X_3	1	0.44	0.1885	2.02	1	0.05	0.8885	0.02	1	230.28	0.0525	4.98
Interaction												
X_1X_2	1	31.64	<0.0001	145.20	1	0.21	0.7734	0.09	1	617.76	0.0053	13.38
X_1X_3	1	0.39	0.2129	1.80	1	0.13	0.8241	0.05	1	50.50	0.3230	1.09
X_2X_3	1	0.18	0.3909	0.81	1	1.56	0.4444	0.64	1	37.41	0.3915	0.81
Quadratic												
X_1^2	1	23.86	<0.0001	109.49	1	22.06	0.0147	9.06	1	3813.79	<0.0001	82.58
X_2^2	1	40.99	<0.0001	188.11	1	56.40	0.0010	23.16	1	2182.32	<0.0001	47.26
X_3^2	1	6.93	0.0003	31.81	1	6.91	0.1264	2.84	1	659.91	0.0043	14.29
Model	9	152.82	<0.0001	77.92	9	268.37	0.0005	12.25	9	8083.80	<0.0001	19.47
Lack of fit	4	1.37	0.1363	2.91	4	15.94	0.1096	3.33	4	403.73	0.0005	42.38
Summary of fit												
R^2	0.9873				0.9245				0.9512			
R^2_{adj}	0.9747				0.8490				0.9023			
C.V.%	2.33				10.13				13.65			

Note: [a] Degree of freedom, [b] Sum of squares.

$$Y_2 = -18.376 + 0.402X_1 + 0.746X_2 + \\ + 0.165X_3 - 0.001X_2X_3 - 0.003X_1^2 - \\ - 0.006X_2^2 - 0.001X_3^2 \quad (3)$$

According to the ANOVA data consolidated in Table 3, the R^2 computed for the TFC model was 0.9245. This metric, reflecting the proportion of total variance accounted for by the regression, confirms that the mathematical framework fits the experimental system well. Furthermore, the corresponding R^2_{adj} for this target output exceeded the 0.80 threshold. This elevated value demonstrates a close, reliable concordance between the empirical datasets gathered in the laboratory and the theoretical projections mapped by the quadratic equations (Azahar et al., 2017). Finally, the C.V.% remained relatively low, hovering at approximately 10%, which verifies a high degree of experimental reproducibility for the investigated extraction system (Filip et al., 2017).

Statistical evaluation of the RSC indicates that all independent processing variables exerted a positive influence via their linear terms, while conversely exhibiting a negative impact through their corresponding second-order quadratic components. The microwave-assisted recovery of RSC from *M. oleifera* L. was primarily dictated by the linear coefficient of the L/S ratio (X_2), supplemented by the quadratic terms of EtOH concentration (X_1^2), L/S ratio (X_2^2), and processing time (X_3^2), all of which reached statistical significance ($p < 0.05$). In contrast, the linear parameters for EtOH fraction (X_1) and extraction duration (X_3), alongside all cross-product interactive pairings (X_1X_2, X_1X_3, and X_2X_3), were determined to be statistically negligible ($p > 0.05$). Furthermore, as consolidated in Table 3, both the R^2 and R^2_{adj} values surpassed the 0.90 threshold, validating the mathematical adequacy of the regression framework for this target output. Based on these relationships, the final predictive polynomial expression established for RSC (Equation 4) is presented below:

$$Y_3 = -176.565 + 8.874X_1 + 4.149X_2 + \\ + 1.548X_3 - 0.044X_1X_2 - 0.008X_1X_3 + \\ + 0.004X_2X_3 - 0.167X_1^2 - 0.040X_2^2 - 0.008X_3^2 \quad (4)$$

The ANOVA data compiled in Table 3 demonstrated that specific coefficients within the second-order polynomial equations exerted a highly pronounced impact on their respective target responses, as evidenced by low p-values coupled with correspondingly elevated F-statistics (Azahar et al., 2017). Notably, the overall quadratic models developed for TPC, TFC, and RSC consistently exhibited p-values well below the 0.05 threshold, verifying that these regression frameworks are statistically significant and capable of accurately mapping the underlying mass-transfer and extraction dynamics (Yang and Hong, 2018). The distinct variations observed in the significance patterns among the independent parameters suggest that the ideal extraction coordinates are non-identical for each individual phytochemical class. This divergence is fundamentally driven by the unique physiochemical attributes of the target compounds, alongside the structural and matrix complexity inherent to the botanical tissue (Chatepa et al., 2025).

Impact of operational variables on TPC, TFC, and RSC recovery

As previously mentioned, EtOH concentration, L/S ratio, and extraction time were the critical independent variables chosen to determine the optimal conditions for extracting polyphenolic compounds from *M. oleifera* L.. The three-dimensional response surface plots (Figures 1–3) show the effects of these extraction conditions on TPC, TFC, and RSC. The response surface plots of the model were generated by varying two variables within the experimental range under investigation while holding the other variables at their central levels.

The amount of TPC (Y_1) recovered from *M. oleifera* L. via a single MAE procedure spanned a range from 13.0 to 23.1 mg GAE/g. This variation was observed across the experimental range of the independent variables: EtOH concentration (X_1), from 20% to 60% (v/v); L/S ratio (X_2), from 20:1 to 60:1 mL g^{-1}; and extraction time (X_3), from 60 to 120 s. The maximal TPC was recorded under the extraction conditions (X_1, X_2, X_3) of (40%, 40:1 mL g^{-1}, 90 s), while the minimal TPC was observed at (20%, 20:1 mL g^{-1}, 120 s). The specific influence of these variables and the interactions on the responses is visually represented in Figure 1.

Figure 1a illustrates the combined effect of EtOH concentration (X_1) versus L/S ratio (X_2) on the TPC (Y_1), with the extraction time (X_3) fixed at 90 s. The response surface plot revealed that at the lowest L/S ratio (20 mL g^{-1}), adding EtOH to water significantly increased the recovery of polyphenolics from *M. oleifera* L., which peaked at approximately 40–60% (v/v) and then gradually decreased as the EtOH concentration exceeded 80% (v/v). A similar trend was observed in the study by Rodríguez-Pérez et al. (2015), where the concentration of EtOH increased from 50% to 70%, resulting in a half decrease in TPC recovery. Nevertheless, to achieve a TPC yield greater than 20 mg GAE/g at a low EtOH concentration, a large amount of solvent (i.e., a high L/S ratio) was required. This difference in extraction efficiency can be attributed to the different polarities of the bioactive constituents and their interaction with the extraction solvent (Rodríguez-Pérez et al., 2015). As phenolic compounds are polar molecules, the TPC yield generally increased with greater water content in line with the "like dissolves like" principle. A high concentration of EtOH can be detrimental to extraction, as it causes protein denaturation, preventing the proper dissolution of polyphenols and thus limiting the extraction rate (Dahmoune et al., 2015).

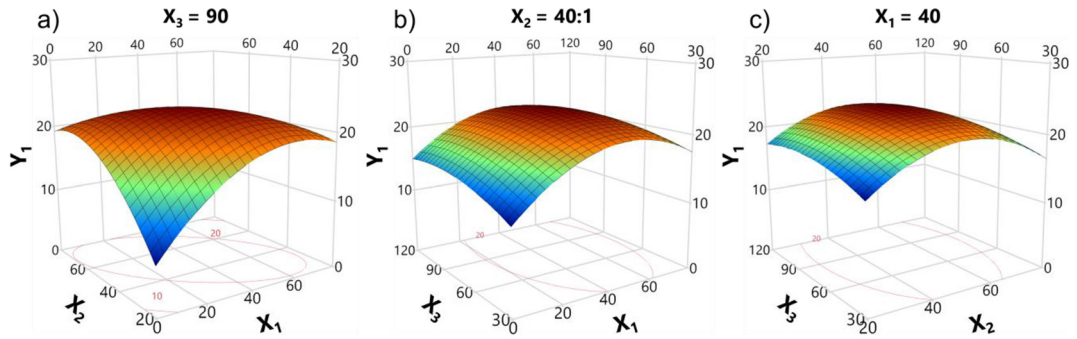

Figure 1. Response surface plots for the effects of EtOH concentration (X_1), L/S ratio (X_2), and extraction time (X_3) on TPC (Y_1) of the *M. oleifera* L. extract

However, the presence of EtOH is essential because it provides synergistic benefits by accelerating mass transfer between the solid and liquid phases, increasing the permeability of the plant tissue, and disrupting the binding of solutes to the plant matrix (Bouras et al., 2015). The balance of effects explains why the maximum TPC was ultimately recorded using an optimal 40:60 (v/v) EtOH-water mixture. This observation of peak extraction efficiency at a moderate EtOH concentration is highly consistent with results reported in the literature for other matrices, such as 42% EtOH for *Myrtus communis* L. leaves (Dahmoune et al., 2015), 42% EtOH for *Nephelium Lappaceum* L. peels (Huynh et al., 2025), and 48% EtOH for grapefruit peels (Islam et al., 2023).

The response surface plot, as a function of EtOH concentration (X_1) versus extraction time (X_3) at a constant L/S ratio (X_2) of 40 mL g^{-1}, is presented in Figure 1b. It was observed that increasing both parameters initially results in a higher phenolic content, reaching a maximum TPC at an EtOH concentration of 40% (v/v) and a relatively short irradiation time of approximately 90 s. However, extending the extraction time to 120 s did not improve the yield; instead, the TPC value gradually dropped. This phenomenon is explained by the rapid attainment of the extraction equilibrium, in which the solute concentration in the solid matrix equals that in the bulk solution after a certain time. This finding is consistent with Fick's second law of diffusion (Azahar et al., 2017; Mokrani and Madani, 2016) and demonstrates a key advantage of the MAE method (reduced extraction time, reduced solvent usage, and increased extraction yield) (Gharsallah et al., 2023). The subsequent decrease in TPC is attributed to the oxidation or degradation of the phenolic compounds resulting from prolonged microwave irradiation (Tomasi et al., 2023).

The response surface plot in Figure 1c illustrates the effect of L/S ratio (X_2) and extraction time (X_3), with the EtOH concentration (X_1) maintained at 40% (v/v). The data show that increasing both parameters initially induced a higher TPC. Considering the extraction time results, an L/S ratio of 50 mL g^{-1} yielded the highest TPC as compared with 40 mL g^{-1} or 60 mL g^{-1}. This observation aligns with the mechanism proposed by Zhu et al. (2015), in which an increase in L/S ratio enhances extraction by creating a significant concentration difference between the interior plant cells and the bulk solution, thereby promoting the faster diffusion of active compounds. However, a further increase in L/S ratio can absorb more microwave radiation and extend the diffusion distance, which negatively impacts the yield of active compounds (Alara et al., 2018). In contrast, using a low L/S ratio is also detrimental, as the solution rapidly reaches saturation. This restricts the solvent's ability to dissolve additional material, leaving some polyphenolics trapped within the solid matrix and rendering the overall extraction process inefficient (Nguyen-Doan et al., 2024).

The assessment of the TFC extraction capacity was performed using the same operational parameters previously mentioned during the investigation of the TPC. The experimental results demonstrated that the TFC extracted from *M. oleifera* L. varied significantly across the tested conditions, with yields ranging from 7.0 to 20.2 mg RE/g. The maximal TFC yield was recorded under the operational condition (X_1, X_2, X_3) set (60%, 60:1 mL g^{-1}, 60 s), while the minimal TFC yield was observed at (20%, 20:1 mL g^{-1}, 60 s). The influence of the extraction variables and their interaction effects on the TFC is visually depicted in Figure 2.

The effect of individual extraction parameters on TFC generally follows a similar trend to that for TPC, with an initial increase in the variable leading to a higher TFC. The maximal TFC was experimentally determined at an L/S ratio (X_2) of approximately 50 mL g^{-1} (refer to Figures 2a and 2c) and an extraction time of 90 s (refer to Figures 2b and 2c). However, the response surface analysis (Figure 2a) for the interaction between EtOH concentration (X_1) and L/S ratio (X_2) at a fixed extraction time (X_3) of 90 s showed that the peak TFC was observed at approximately 60% EtOH concentration (v/v). This observed variation in the optimal EtOH concentration is primarily attributable to the distinct solubilities and extraction efficiencies of the components under the tested solvent conditions. Mechanistically, the increase in EtOH concentration promotes the breakdown of the cell membrane, which enhances the permeability of the solvent into the solid matrix and facilitates the release of the targeted compounds (Azahar et al., 2017). This finding is consistent with previous studies that identified the optimal conditions for flavonoid extraction from *Cayratia trifolia* L. berries (Nguyen-Doan et al., 2024) and *Docynia indica* (Wall.) Decne. (Le et al., 2019) were obtained using 60% and 65% (v/v) EtOH as solvents, respectively.

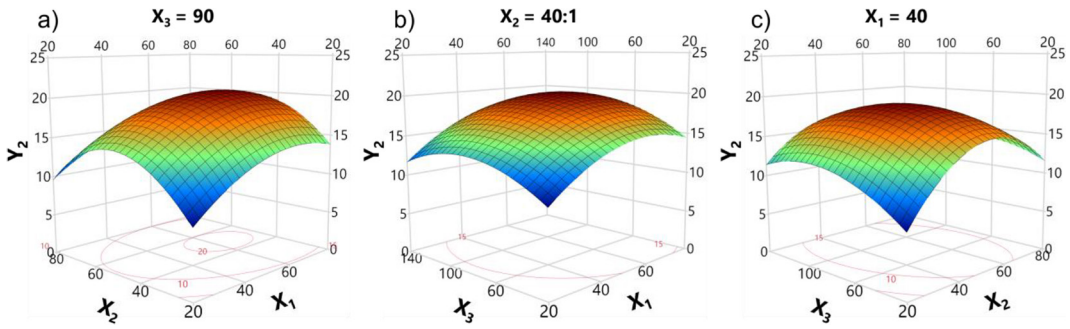

Figure 2. Response surface plots for the effects of EtOH concentration (X_1), L/S ratio (X_2), and extraction time (X_3) on TFC (Y_2) of the *M. oleifera* L. extract

Previous studies indicate that reducing sugars, which possess a free aldehyde or ketone functional group, exhibit a strong affinity for aqueous solvents (Lama-Calvente et al., 2024). Consequently, the optimal extraction of the RSC (Y_3) from *M. oleifera* L. was systematically explored by adjusting the EtOH concentration (X_1) across a range of 10 to 30% (v/v), while the L/S (X_2) and the extraction time (X_3) were held constant at 20–60 mL g^{-1} and 60–120 s, respectively. This controlled experimentation revealed that the RSC yield varied significantly, spanning from 21.1 to 77.2 mg GE/g. The maximal recovery was attained under the specific parameters (X_1, X_2, X_3) of (20%, 40:1 mL g^{-1}, 90 s), while the minimal recovery was recorded at (37%, 40:1 mL g^{-1}, 90 s). Figure 3 illustrates the influence of these extraction variables and their interactive effects on the RSC.

As mentioned above, reducing sugars exhibit solubility in a polar solution, aligning with the principle of "like dissolves like". Pure water is suboptimal for the efficient extraction of these compounds from plant materials, while a combination of solvents may be more effective in facilitating the extraction of compounds with different polarities that remain in the leaves (Gharsallah et al., 2023; Yirgu et al., 2021). The incorporation of EtOH is critical to the extraction process, as it is known to promote disruption of the cell membrane, enhancing solvent permeability into the solid matrix (Azahar et al., 2017) and allowing effective extraction of reducing sugars released from polysaccharides or lignin. While the solvent mixture retains its capacity to solubilize reducing sugars at low EtOH concentrations, excessively high EtOH concentrations are detrimental, leading to diminished yield due to potential dissolution or denaturation of the reducing sugars. As illustrated in Figures 3a and 3b, the optimal EtOH concentration (X_1) for maximizing the extraction of RSC (Y_3) falls within the range of approximately 15% to 20% (v/v).

As shown in Figures 3a and 3c, the optimal L/S (X_2) for maximizing RSC recovery was approximately 50 mL g^{-1}. This proportion is consistent with the optimal ratios for both TPC and TFC, indicating that 50 mL g^{-1} in this study is generally suitable for extracting various extracts from *M. oleifera* L. The negligible variation in the optimal L/S among various target compounds suggests that the extraction process is more influenced by the inherent characteristics of the plant material than by the specific compound being targeted, which aligns with a previous study of Yang and Hong (2018). However, the extraction time required to reach maximum RSC was longer, approximately 100 s (Figure 3b and 3c), than for TPC and TFC. This variability can be attributed to the low EtOH concentration, which requires a longer duration to effectively disrupt the membrane and cell wall, thereby facilitating the release of the target reducing sugars. Despite this slight difference, an extraction time of 100 s remains very short, demonstrating the high efficiency of the MAE method.

Response optimization, experimental verification of predictive models, and phytochemical-antioxidant activity correlations

By solving the second-order polynomial expressions (Equations 2–4) generated via RSM, the ideal parameter combinations for maximizing the target outputs were established, with the specific numerical coordinates summarized in Table 4. At these optimized settings, the mathematical models projected maximum theoretical recovery

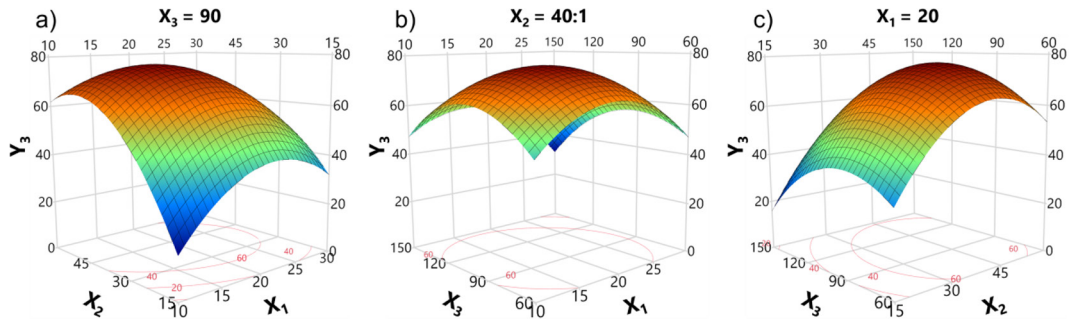

Figure 3. Response surface plots for the effects of EtOH concentration (X_1), L/S ratio (X_2), and extraction time (X_3) on RSC (Y_3) of the *M. oleifera* L. extract

thresholds of 23.2 mg GAE/g for TPC, 20.5 mg RE/g for TFC, and 77.5 mg DE/g for RSC. To rigorously assess the predictive fidelity of these quadratic frameworks, empirical verification trials were executed in triplicate. The resulting mean experimental yields converged closely at 23.5 mg GAE/g for TPC, 20.8 mg RE/g for TFC, and 76.3 mg DE/g for RSC. The relative error (RE) values calculated between the theoretical projections and empirical datasets consistently remained below 5%. This negligible residual discrepancy demonstrates that the developed RSM regression models possess good statistical adequacy and high forecasting reliability for mapping and controlling the independent extraction variables during the MAE of *M. oleifera* L. bioactives.

The radical scavenging performance of the *M. oleifera* L. extracts, fundamentally driven by the co-extracted polyphenolic and flavonoid fractions, was evaluated utilizing the DPPH assay. Under processing parameters optimized for individual yield outputs, the antioxidant capacity consistently maintained elevated plateaus ranging from 5.03 to 5.20 mg TE/g in tandem with maximized TPC and TFC recoveries. Conversely, a pronounced contraction to 2.84 mg TE/g was observed when applying the optimal extraction coordinates tailored exclusively for RSC yields (Table 4). This behavioral divergence highlights the fundamental kinetic and mechanistic mismatches occurring between these distinct solute classes and the DPPH radical probe. Because the DPPH decolorization pathway operates via parallel hydrogen-atom transfer (HAT) and single-electron transfer (SET) mechanisms, it selectively targets the highly labile aromatic hydroxyl functionalities characteristic of polyphenols, rather than the aliphatic hydroxyl orientations present on reducing sugars (Shahidi and Samarasinghe, 2025). This clear mechanistic preference explains the robust statistical alignment connecting antioxidant capacities directly to the total polyphenol density within the matrix. As a result, maintaining a moderate EtOH fraction in the extractant mixture represents the most effective strategy to ensure high antioxidant values, a trend that directly mirrors the optimized extraction zones established for TPC and TFC. These empirical dynamics strongly corroborate previous extraction models documented by Bouras et al. (2015), Filip et al. (2017), and Huynh et al. (2025). The interactive dependencies linking the

Table 4. Predicted versus empirical response values for the validated optimal extraction parameters

Response variable	Optimal conditions [a]			Responses			Antioxidant activity (mg TE/g) [b,d]
	X_1 (%, v/v)	X_2 (mL g^{-1})	X_3 (s)	Predicted value	Experimental value [b]	RE (%) [c]	
Y_1 (mg GAE/g)	38.8 (40)	51.2 (50)	84.7 (85)	23.2	23.5 ± 0.9	1.3	5.03 ± 0.03
Y_2 (mg RE/g)	63.1 (60)	50.6 (50)	89.4 (90)	20.5	20.8 ± 0.7	1.4	5.20 ± 0.04
Y_3 (mg DE/g)	18.0 (20)	46.2 (45)	101.4 (100)	77.5	76.3 ± 1.9	1.6	2.84 ± 0.23

Note: [a] The experimental conditions are presented in brackets, [b] An average value ± standard deviation (for three replicates), [c] RE (%) = (|the experimental value – the predicted value|/the experimental value)·100, [d] The antioxidant capacity is assessed under the optimal conditions.

modeled antioxidant profiles to both TPC and TFC distributions were mathematically mapped and are visualized in Figure 4.

A robust, upward linear relationship was observed between AA and TPC, yielding a Pearson correlation coefficient (r) of 0.88 and a determination coefficient (R^2) of 0.78. This close alignment mirrors baseline values documented for distinct regional flora, such as Nepalese botanical extracts (r = 0.866 and R^2 = 0.750) (Khatri and Chhetri, 2020). Correspondingly, mapping AA against TFC revealed comparable statistical pairings (r = 0.85, R^2 = 0.73). While the marginally elevated regression metrics for the TPC dataset imply that the radical-trapping efficacy depends slightly more heavily on the total phenolic fraction, this minor variation lack statistical significance, indicating that these distinct polyphenolic subsets function synergistically to drive the cumulative antioxidant performance. From a mechanistic standpoint, these organic molecules act as highly efficient hydrogen-atom or single-electron donors. Their specific structural chemistry, characterized by conjugated aromatic systems and hydroxyl substitution patterns, is optimized for the rapid stabilization of radical species. Chromatographic profiles of *M. oleifera* L. extracts frequently highlight an abundance of key glycosylated flavonoids, specifically rutin and quercitrin, both of which possess well-documented, high-efficiency radical scavenging pathways (Bennour et al., 2021).

Nevertheless, literature indicates that the numerical alignment between total phenolic metrics and overall antioxidant assays frequently exhibits non-linear fluctuations. This divergence stems directly from the structural heterogeneity of the target fractions; the total extractable phenolic pool comprises an intricate constellation of biomolecules characterized by divergent polarities, spatial orientations, and molecular weights (Molole et al., 2022). Consequently, these distinct structural profiles dictate individual mass-transfer kinetics and solvent affinities, giving rise to localized disparities when mapping scavenging responses against specific polyphenolic subsets. Furthermore, as previously documented, the ultimate correlation coefficients are not merely a function of absolute phytochemical payloads. Instead, they reflect the collective synergistic or antagonistic interactions taking place within the native matrix, alongside the specific thermodynamic and kinetic constraints of the chosen *in vitro* radical scavenging assay (Parikh and Patel, 2018). Ultimately, these multivariable dynamics corroborate the established consensus that *M. oleifera* L. leaf tissue functions as a potent natural antioxidant reservoir, exhibiting a strong, predictable linear trend between its cumulative polyphenol content and overall radical scavenging efficacy (Chatepa et al., 2025).

The empirical data consolidated in Table 5 confirm that utilizing aqueous ethanol as an extractant yields high TPC recoveries, aligning closely with established extraction trends documented in the literature (Gao et al., 2025; Makkiyah et al., 2024; Rodríguez-Pérez et al., 2015). Specifically, the TFC value isolated in this work (20.8 mg RE/g) compares favorably and shows statistical parity with the 22.5 mg RE/g threshold achieved by Chatepa et al. (2025). While target yields remain comparable across these frameworks, the

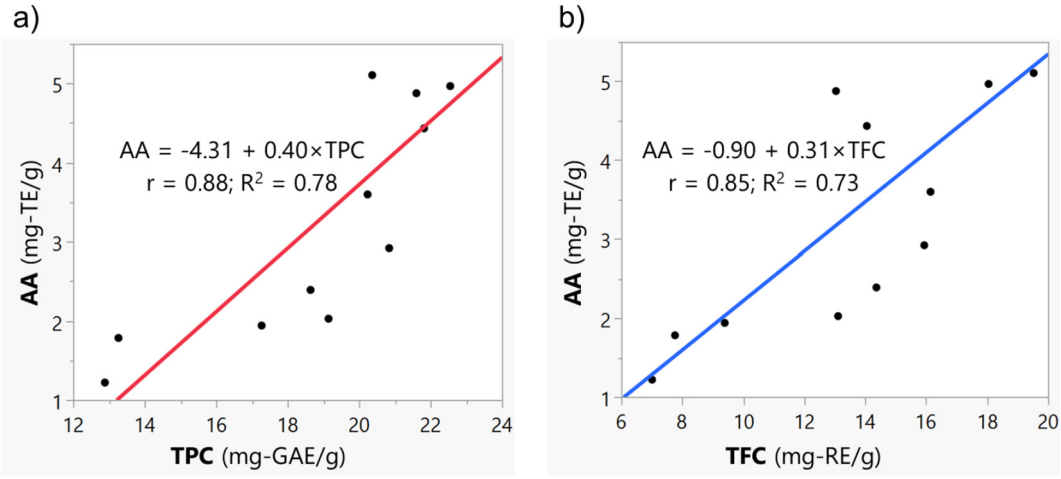

Figure 4. Regression analysis plots showing the statistical alignment of AA against: (a) TPC and (b) TFC

Table 5. Evaluation of the current MAE performance against literature benchmarks for *M. oleifera* L. leaf extracts

Methods	Solvents	Extraction conditions	TPC (mg GA/g)	References
Maceration	EtOH (50%)	L/S = 50:1 60 min	27 ± 2	Rodríguez-Pérez et al. (2015)
	EtOH (70%)		24.3 ± 0.3	
UAE (1st extraction)	EtOH (50%)	L/S = 50:1 15 min	24 ± 3	
	EtOH (70%)		12.6 ± 0.2	
	EtOH (50%)	L/S = 40:1 60 min	27.09 ± 0.33	Gao et al. (2025)
MAE	EtOH (60%)	L/S = 15:1 180 s	17.9	Makkiyah et al. (2024)
	EtOH (40%)	L/S = 50:1 85 s	23.5 ± 0.9	This study

current MAE approach offers distinct competitive advantages, establishing itself as a superior methodology by virtue of its dramatically compressed extraction windows, lowered operational expenditure, reduced environmental footprint, and enhanced kinetic efficiency. Collectively, these comparative profiles reinforce the fact that high polyphenol concentrations represent a foundational phytochemical hallmark of *M. oleifera* L. leaves. Nevertheless, because plant matrices exhibit localized compositional variations dictated by geographic origin, executing a rigorous, site-specific optimization of processing parameters remains a mandatory prerequisite to unlock the maximum bioactive potential of the biomass.

CONCLUSIONS

In this work, RSM driven by a CCD was successfully applied to optimize and maximize the extraction yields of TPC, TFC, and RSC from *M. oleifera* L. leaves via a microwave-assisted framework. The complex, interactive relationships between the operational parameters (ethanol concentration, extraction duration, and liquid-to-solid ratio) and the target response variables were comprehensively mapped using three-dimensional response surface plots. Variance analysis demonstrated that the quadratic impacts of these independent factors were highly significant across all evaluated responses, with the sole exception of the quadratic extraction time parameter for TFC; conversely, the linear and cross-product interaction impacts displayed varying degrees of significance depending on the specific target. The established second-order polynomial models showed good predictive capacity for the relative responses and successfully defined the optimal processing windows. Furthermore, a strong linear correlation was confirmed between the radical-scavenging activity (AA) of the isolated fractions and their corresponding TPC and TFC values. Taken together, these findings validate MAE as a highly efficient, green, and sustainable strategy for isolating polyphenol-rich fractions from *M. oleifera* L. matrixes. Ultimately, tailoring and finely tuning the specific MAE operational settings allows for the targeted maximization of distinct bioactive classes, thereby paving the way for their full-scale integration into industrial applications.

Acknowledgements

This research was (partially) supported by Murata Science and Education Foundation. We also acknowledge Ho Chi Minh City University of Technology (HCMUT), VNU-HCM for supporting this study.

REFERENCES

1. Alara, O.R., Abdurahman, N.H., Ukaegbu, C.I. (2021). Extraction of phenolic compounds: A review. *Current Research in Food Science*, *4*, 200–214. https://doi.org/10.1016/j.crfs.2021.03.011
2. Alara, O.R., Abdurahman, N.H., Olalere, O.A. (2018). Optimization of microwave-assisted extraction of flavonoids and antioxidants from *Vernonia amygdalina* leaf using response surface methodology. *Food and Bioproducts Processing*, *107*, 36–48. https://doi.org/10.1016/j.fbp.2017.10.007
3. Al-Shalabi, R. & Samad, N.A. (2024). *Moringa oleifera* extraction, isolation, quantification and its application in functional foods: A review. *Australian Herbal Insight*, *7*(1), 9958. https://doi.org/10.25163/ahi.719958
4. Azahar, N.F., Gani, S.S.A., Mokhtar, N.F.M. (2017). Optimization of phenolics and flavonoids extraction

conditions of *Curcuma Zedoaria* leaves using response surface methodology. *Chemistry Central Journal*, *11*, 96. https://doi.org/10.1186/s13065-017-0324-y

5. Bennour, N., Mighri, H., Bouhamda, T., Mabrouk, M., Apohan, E., Yesilada, O., Küçükbay, H., Akrout, A. (2021). *Moringa oleifera* leaves: could solvent and extraction method affect phenolic composition and bioactivities?. *Preparative Biochemistry and Biotechnology*, *51*(10), 1018-1025. https://doi.org/10.1080/10826068.2021.1891550
6. Bouras, M., Chadni, M., Barba, F.J., Grimi, N., Bals, O., Vorobiev, E. (2015). Optimization of microwave-assisted extraction of polyphenols from *Quercus* bark. *Industrial Crops and Products*, *77*, 590–601. https://doi.org/10.1016/j.indcrop.2015.09.018
7. Chatepa, L.E.C., Mwamatope, B., Chikowe, I., Ntholo, M., Masamba, K.G. (2025). Extraction of phytoconstituents and antioxidant properties from *Moringa oleifera* L. leaves and seeds from Malawi: A comparative study using deep eutectic and conventional solvents. *Food and Humanity*, *4*, 100635. https://doi.org/10.1016/j.foohum.2025.100635
8. Chokoe, T.A., Shinga, M.H., Silue, Y., Mpai, S., Fawole, O.A., Ndhlala, A.R. (2025). Phenolic metabolite profiling of *Moringa oleifera* Lam. waste under different drying methods and extraction solvents. *South African Journal of Botany*, *184*, 182–192. https://doi.org/10.1016/j.sajb.2025.06.005
9. Dahmoune, F., Nayak, B., Moussi, K., Remini, H., Madani, K. (2015). Optimization of microwave-assisted extraction of polyphenols from *Myrtus communis* L. leaves. *Food Chemistry*, *166*, 585–595. https://doi.org/10.1016/j.foodchem.2014.06.066
10. Filip, S., Pavlić, B., Vidović, S., Vladić, J., Zeković, Z. (2017). Optimization of microwave-assisted extraction of polyphenolic compounds from *Ocimum basilicum* by response surface methodology. *Food Analytical Methods*, *10*, 2270–2280. https://doi.org/10.1007/s12161-017-0792-7
11. Gao, Q., Liu, X., Shi, J., Li, L., Sun, B. (2025). Polyphenols in different parts of *Moringa oleifera* Lam.: Composition, antioxidant and neuroprotective potential. *Food Chemistry*, *475*, 143207. https://doi.org/10.1016/j.foodchem.2025.143207
12. Gharsallah, K., Rezig, L., Rajoka, M.S.R., Mehwish, H.M., Ali, M.A., Chew, S.C. (2023). *Moringa oleifera:* Processing, phytochemical composition, and industrial applications. *South African Journal of Botany*, *160*, 180–193. https://doi.org/10.1016/j.sajb.2023.07.008
13. Hamid, M.H.A., Yusoff, M.H.M., Rosazlina, R., Shafie, M.H. (2025). A review on *Moringa oleifera polysaccharides*: Extraction, purification, structure-activity, bioactivities and application. *International Journal of Biological Macromolecules*, *323*(1), 147089. https://doi.org/10.1016/j.ijbiomac.2025.147089
14. Hu, Y., Yan, B., Chen, Z.S., Wang, L., Tang, W., Huang, C. (2022). Recent technologies for the extraction and separation of polyphenols in different plants: A review. *Journal of Renewable Materials*, *10*(6), 1471–1490. https://doi.org/10.32604/jrm.2022.018811
15. Huynh, T.B., Do, T.A.S., Tran, T.K.A., Dang-Bao, T. (2025). Optimization of microwave-assisted extraction of polyphenolics from rambutan (*Nephelium Lappaceum* L.) peels using response surface methodology and central composite design. *Engineering, Technology & Applied Science Research*, *15*(3), 22431–22436. https://doi.org/10.48084/etasr.10570
16. Islam, M., Malakar, S., Dwivedi, U., Kumar, N., Prabakar, P.K., Kishore, A., Kumar, A. (2023). Impact of different drying techniques on grapefruit peels and subsequent optimization of ultrasonic extraction conditions for bioactive compounds. *Journal of Food Process Engineering*, *46*(6), e14331. https://doi.org/10.1111/jfpe.14331
17. Izadiyan, P., Hemmateenejad, B. (2016). Multi-response optimization of factors affecting ultrasonic assisted extraction from Iranian basil using central composite design. *Food Chemistry*, *190*, 864–870. https://doi.org/10.1016/j.foodchem.2015.06.036
18. Khatri, D., Chhetri, S.B.B. (2020). Reducing sugar, total phenolic content, and antioxidant potential of nepalese plants. *BioMed Research International*, *2020*, 7296859. https://doi.org/10.1155/2020/7296859
19. Lam, H.H., Nguyen, T.M.T., Do, T.A.S., Dinh, T.H., Dang-Bao, T. (2021). Quantification of total sugars and reducing sugars of dragon fruit-derived sugar-samples by UV-Vis spectrophotometric method. *IOP Conference Series: Earth and Environmental Science*, *947*, 012041. https://doi.org/10.1088/1755-1315/947/1/012041
20. Lama-Calvente, D.D., Fernández-Rodríguez, M.J., Garrido-Fernández, A., Borja, R. (2024). Process optimization of the extraction of reducing sugars and total phenolic compounds from the invasive alga *Rugulopteryx okamurae* by response surface methodology (RSM). *Algal Research*, *80*, 103500. https://doi.org/10.1016/j.algal.2024.103500
21. Le, X.D., Nguyen, M.C., Vu, D.H., Pham, M.Q., Pham, Q.L., Nguyen, Q.T., Nguyen, T.A., Pham, V.T., Bach, L.G., Nguyen, T.V., Tran, Q.T. (2019). Optimization of microwave-assisted extraction of total phenolic and total flavonoid contents from fruits of *Docynia indica* (Wall.) decne. Using Response Surface Methodology. *Processes*, *7*(8), 485. https://doi.org/10.3390/pr7080485
22. Makkiyah, F.A., Pradana, D.L.C., Putra, R.P., Nurcholis, W. (2024). Optimization microwave-assisted extraction of *Moringa oleifera* leaves using response surface methodology focused on extracting phenolic and flavonoid with antioxidant activity. *Tropical Journal of Natural Product Research*, *8*(6), 7474–7482. https://doi.org/10.26538/tjnpr/v8i6.21

23. Mokrani. A., Madani, K. (2016). Effect of solvent, time and temperature on the extraction of phenolic compounds and antioxidant capacity of peach (*Prunus persica* L.) fruit. *Separation and Purification Technology*, *162*, 68–76. https://doi.org/10.1016/j.seppur.2016.01.043
24. Molole, G.J., Gure, A., Abdissa, N. (2022). Determination of total phenolic content and antioxidant activity of *Commiphora mollis* (Oliv.) Engl. Resin. *BMC Chemistry*, *16*, 48. https://doi.org/10.1186/s13065-022-00841-x
25. Nguyen-Doan, M.A., Huynh, T.B., Tu, Q.D., Nguyen, M.T.K., Do, T.A.S., Lam, H.H., Dang-Bao, T. (2024). Drying method-affected polyphenolic contents: a microwave-assisted extraction from *Cayratia trifolia* L. berry. *IOP Conference Series: Earth and Environmental Science*, *1340*(1), 012027. https://doi.org/10.1088/1755-1315/1340/1/012027
26. Parikh, B., Patel, V.H. (2018). Total phenolic content and total antioxidant capacity of common Indian pulses and split pulses. *Journal of Food Science and Technology*, *55*, 1499–1507. https://doi.org/10.1007/s13197-018-3066-5
27. Peng, W., Wang, L., Wang, X., Wang, Y., Wang, W., Huang, J., Zhou, R., Chen, C., Bo, R., Liu, M., Li, J. (2025). Efficient polyphenol extraction from *Moringa oleifera* Lam. leaves using natural deep eutectic solvents: COSMO-RS screening, ANN-GA optimization and antioxidant activity evaluation. *LWT*, *223*, 117687. https://doi.org/10.1016/j.lwt.2025.117687
28. Pimentel-Moral, S., Borrás-Linares, I., Lozano-Sánchez, J., Arráez-Román, D., Martínez-Férez, A., Segura-Carretero, A. (2018). Microwave-assisted extraction for *Hibiscus sabdariffa* bioactive compounds. *Journal of Pharmaceutical and Biomedical Analysis*, *156*, 313–322. https://doi.org/10.1016/j.jpba.2018.04.050
29. Rodríguez-Pérez, C., Quirantes-Piné, R., Fernández-Gutiérrez, A., Segura-Carretero, A. (2015). Optimization of extraction method to obtain a phenolic compounds-rich extract from *Moringa oleifera* Lam leaves. *Industrial Crops and Products*, *66*, 246–254. https://doi.org/10.1016/j.indcrop.2015.01.002
30. Shahidi, F., and Samarasinghe, A. (2025). How to assess antioxidant activity? Advances, limitations, and applications of in vitro, in vivo, and ex vivo approaches. *Food Production, Processing and Nutrition*, *7*, 50. https://doi.org/10.1186/s43014-025-00326-z
31. Szopa, D., Wróbel, P., Witek-Krowiak, A. (2024). Enhancing polyphenol extraction efficiency: A systematic review on the optimization strategies with natural deep eutectic solvents. *Journal of Molecular Liquids*, *404*, 124902. https://doi.org/10.1016/j.molliq.2024.124902
32. Teclegeorgish, Z.W., Aphane, Y.M., Mokgalaka, N.S., Steenkamp, P., Tembu, V.J. (2021). Nutrients, secondary metabolites and anti-oxidant activity of *Moringa oleifera* leaves and Moringa-based commercial products. *South African Journal of Botany*, *142*, 409–420. https://doi.org/10.1016/j.sajb.2021.07.008
33. Tomasi, I.T., Santos, S.C.R., Boaventura, R.A.R., Botelho, C.M.S. (2023). Optimization of microwave-assisted extraction of phenolic compounds from chestnut processing waste using response surface methodology. *Journal of Cleaner Production*, *395*, 136452. https://doi.org/10.1016/j.jclepro.2023.136452
34. Vijayalaxmi, S., Jayalakshmi, S.K., Sreeramulu, K. (2014). Polyphenols from different agricultural residues: extraction, identification and their antioxidant properties. *Journal of Food Science and Technology*, *52*, 2761–2769. https://doi.org/10.1007/s13197-014-1295-9
35. Wei, P., Zhang, Y., Wang, Y.Y., Dong, J.F., Lin, Z.H., Li, W., Liu, L., Hu, S.L., Zhang, L., Lou, W.Y., Peng, C. (2023). Efficient extraction and excellent activity of flavonoid from *Moringa oleifera* leaves and its microencapsulation. *LWT*, *184*, 115021. https://doi.org/10.1016/j.lwt.2023.115021
36. Wood, I.P., Elliston, A., Ryden, P., Bancroft, I., Roberts, I.N., Waldron, K.W. (2012). Rapid quantification of reducing sugars in biomass hydrolysates: Improving the speed and precision of the dinitrosalicylic acid assay. *Biomass and Bioenergy*, *44*, 117–121. https://doi.org/10.1016/j.biombioe.2012.05.003
37. Wu, L., Li, L., Chen, S., Wang, L., Lin, X. (2020). Deep eutectic solvent-based ultrasonic-assisted extraction of phenolic compounds from *Moringa oleifera* L. leaves: Optimization, comparison and antioxidant activity. *Separation and Purification Technology*, *247*, 117014. https://doi.org/10.1016/j.seppur.2020.117014
38. Yang, J.X., Hong, G.B. (2018). Optimized extraction for active compounds in *Glossogyne tenuifolia* using response surface methodology. *Journal of Food Measurement and Characterization*, *13*, 663–676. https://doi.org/10.1007/s11694-018-9979-x
39. Yirgu, Z., Leta, S., Hussen, A., Khan, M.M. (2021). Pretreatment and optimization of reducing sugar extraction from indigenous microalgae grown on brewery wastewater for bioethanol production. *Biomass Conversion and Biorefinery*, *13*, 6831–6845. https://doi.org/10.1007/s13399-021-01779-1
40. Zhu, C., Zhai, X., Li, L., Wu, X., Li, B. (2015). Response surface optimization of ultrasound-assisted polysaccharides extraction from pomegranate peel. *Food Chemistry*, *17*, 139–146. https://doi.org/10.1016/j.foodchem.2015.01.022
41. Zhu, Y., Yin, Q., Yang, Y. (2020). Comprehensive investigation of *Moringa oleifera* from different regions by simultaneous determination of 11 polyphenols using UPLC-ESI-MS/MS. *Molecules*, *25*(3), 676. https://doi.org/10.3390/molecules25030676